ORIGINAL ARTICLE

Latin American Journal of Solids and Structures

www.lajss.org

Comparative evaluation of design codes for buckling assessment of a steel spherical shell

Mohd Shahrom Ismail[a], **Jamaluddin Mahmud**[b]*

[a] Jabatan Kejuruteraan Mekanikal, Politeknik Sultan Salahuddin Abdul Aziz Shah, Shah Alam, 40150, Selangor, Malaysia. E-mail: mohdshahrom@psa.edu.my

[b] School of Mechanical Engineering, College of Engineering, Universiti Teknologi MARA, 40450, Shah Alam, Selangor, Malaysia. E-mail: jm@uitm.edu.my

* Corresponding author

https://doi.org/10.1590/1679-78257473

Abstract

This work focuses on the comparative evaluation of the buckling capacity of steel spherical shells subjected to external pressure with existing design codes. The recorded experimental data of buckled spherical shells are compared with the calculated buckling pressure using design codes such as (i) European Convention for Constructional Steelwork (ECCS), (ii) Det Norske Veritas (DnV), (iii) British Standard (PD 5500) and (iv) American Bureau of Shipping (ABS). The selected experimental data are widely used in industrial applications. The experimental data are categorised as 'thin-shell', 'moderate-shell' and 'thick-shell' and reviewed against selected design codes. The comparative analysis clearly shows that the DnV design code with a deviation of 3.6% is well suited to estimate the buckling capacity of 'thick shells", while PD 5500 with a deviation of 9% to 50% is better suited for "medium and thin' shells. On the other hand, statistical analysis shows that PD 5500 is close to 1.0 with the value of COV (i.e., 1.281 and 9.383%). Further analysis of 28 steel spherical shell test data is performed and compared with the plotted curves in the format of PD 5500 and ECCS. The result shows that 3 test data are below the lower limit curve specified in the design guideline for ECCS, indicating that PD 5500 is the more conservative design guideline.

Keywords

Spherical shell; Shell buckling; Design codes; Structural instability; External pressure

Graphical Abstract

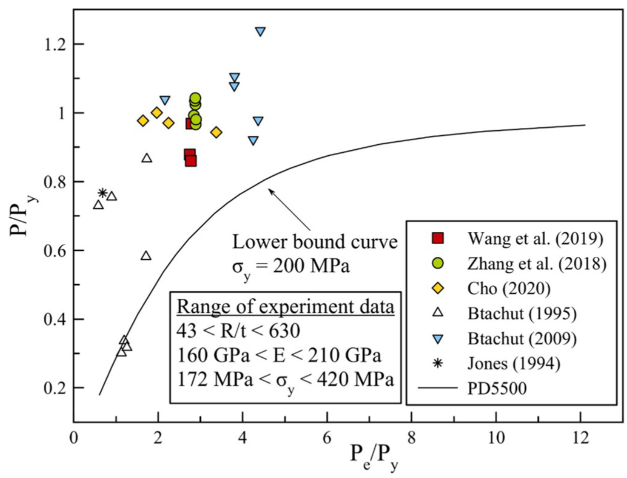

Received: January 17, 2023. In revised form: May 02, 2023. Accepted: May 30, 2023. Available online: June 02, 2023
https://doi.org/10.1590/1679-78257473

1 INTRODUCTION

Steel spherical domes are typically thin-walled structures that are prone to collapse under external pressure, particularly when empty or in use. Previous studies showed discrepancies in the buckling resistance of steel spherical shells between the design method proposed in the European Convention for Constructional Steelwork (ECCS) and the analytical formulas recommended by the British Standard (PD 5500). Spherical shells are commonly used in many engineering design applications. Typically, they are used as a separator in pressure vessels/tanks, as domes to close the ends of cylindrical pressure vessels, or as hatches to cover the access ports of variously shaped pressure vessels in subsea and vacuum vessels (in the chemical industry), aerospace, and civil applications (Ifayefunmi, 2016; Jasion and Magnucki, 2015; Tripathi et al., 2016). In these engineering applications, the shell is most likely subjected to various loading conditions, with external pressure proving to be the most important. The final strength and stability of an externally pressurised spherical shell strongly depend on its shape, material properties, deformations before buckling, and geometric imperfections (Błachut, 2013; Błachut and Magnucki, 2008; Jasion and Magnucki, 2015). For submersible structures, the shell is usually designed to meet the ultimate strength requirements and have some margin of safety to achieve the desired submersion depth (Cho et al., 2020). Success stories in submersible design and development include Jiaolong operated by China NDSC (Błachut, 2018), Shinkai operated by JAMSTEC, Nautile operated by IFREMER, and Consul AS37 operated by the Russian Navy.

In practice, the spherical shell is designed according to the current construction regulations, such as (i) European Convention for Constructional Steelwork (ECCS, 2008), (ii) Det Norske Veritas (DnV, 2013), (iii) British Standard (PD 5500, 2009), and (iv) American Bureau of Shipping (ABS) (American Bureau of Shipping, 2021). These design rules were derived from previous tests, particularly those conducted by the British and American naval research institutions. For example, the design curve in section 3.6 of PD 5500 is derived from the lower bound of the test results. Accordingly, the ECCS design guideline also used the previous theoretical and experimental results to establish the design key. Recently, a series of experiments have been conducted for the case where (i) a spherical shell (Kołodziej and Marcinowski, 2018; Pan et al., 2010; Wang et al., 2020; Zhang et al., 2018, 2017) and (ii) a hemispherical shell (Cho et al., 2020; Zhang et al., 2020, 2019; Zhu et al., 2019) are subjected to external pressure. The tests are considered to be of high quality as they yield a repeatable buckling load for identical models. In general, the spherical shell is categorised as full, deep, and thin (Wagner et al., 2018). The functionally graded (FG) three-layered conical shell and cone-cylinder transition under external pressure has both been the subject of recent studies (Sofiyev et al., 2008; Ifayefunmi et al., 2021). Ismail et al. (2015) on the other hand has carried out a statistical investigation on the imperfection effect of the axially-compressed linear composite cylindrical buckling response.

The motivation for this work arises from practical issues related to pressure vessels/tanks and domes used in the industry. It is worth noting that the spherical shell experiences a loss of buckling strength due to deviation in shape caused by manufacturing defects. The present study deals with the evaluation of the buckling capacity of steel spherical shells subjected to external pressure using design codes. Previous studies clearly show that there are discrepancies in the estimation of the buckling strength of steel spherical shells between the industrial design specifications/standards and the experimental results that ranging from 30% to 46% on average, as reported by (Wang, 1967; Ismail, 2023; Cho et al., 2020; Błażejewski and Marcinowski, 2017). Therefore, the purpose of this paper is to discuss and evaluate the uncertainty factors that contribute to the discrepancy in the estimated buckling load of spherical shells in the various design codes. The statistical data of model uncertainty factors in the form of bias and coefficient of variation (COV) are also calculated and further used in a reliability study.

The study is relatively unique since there have been few, if any, studies on this topic. The information, expertise and conclusions of this study are intended to provide insights into the field of design or failure testing of pressure vessels/tanks, submersible structures, vacuum vessels (in the chemical industry), aerospace and civil applications.

2 MATERIALS AND METHOD

2.1 Spherical shell ultimate strength – design code

This section describes the analytical method for calculating the buckling load of a steel spherical shell subjected to external pressure. Figure 1 shows the schematic diagram of a spherical shell subjected to external pressure together with its boundary condition. The terms are denoted as external pressure, P, spherical radius, R, spherical thickness, t, base radius, r, spherical height, H and semi-vertex angle, ϕ.

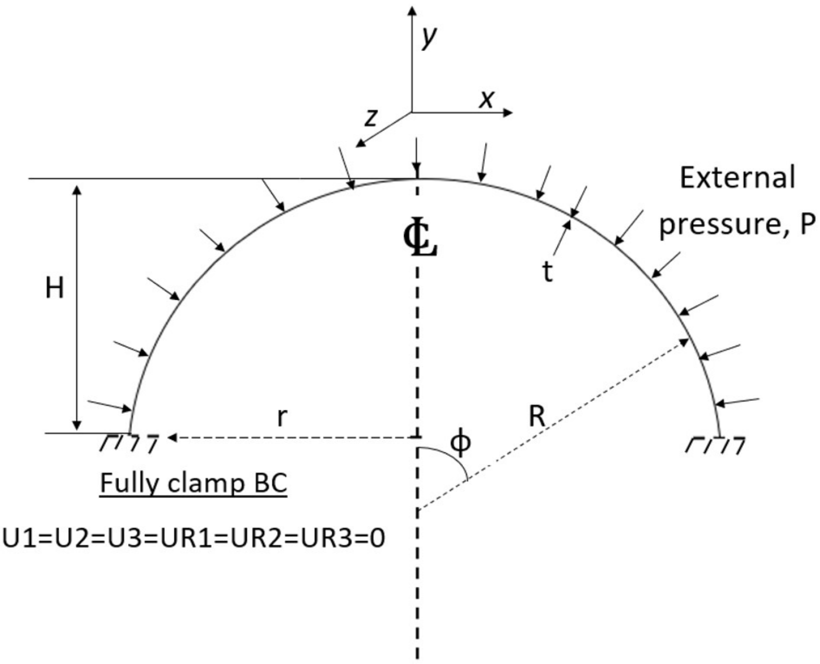

Figure 1: Schematic diagram of Load and boundary condition of the externally pressurised spherical shell

The current design codes namely (i) ECCS, (ii) DnV, (iii) PD 5500, and (iv) ABS, were selected to calculate the spherical shell buckling pressure. The calculated buckling pressure is then benchmarked with the experimental results. This approach is crucial in reviewing the reliability of the existing design codes and is very useful for the initial estimation of the spherical shell buckling load. Normally, the design codes use conventional working stress to determine each mode of failure. Apart from the working stress, the design code is also considering several uncertainties such as safety factor, eccentric boundary condition and load, material hardening and structural imperfection of the tested spherical shell structures. The critical buckling formula, P_{cr} of a complete spherical shell under external pressure was proposed by Zoelly (1915) as shown in equation (1).

$$P_{cr} = \frac{2}{\sqrt{3(1-\nu^2)}}(\frac{t}{R})^2 \quad (1)$$

The terms are defined as the shell radius, R, shell thickness, t and material Poisson's ratio, ν

- The ECCS (2008) design rule estimated the collapse pressure as referred to equations (2) – (3)

$$P_{Rcr} = \frac{2}{\sqrt{3(1-\nu^2)}} c_e E(\frac{t}{R})^2 \quad (2)$$

The factor of C_e is the function of boundary conditions that can be referred to (ECCS, 2008). The factor of C_e covers the buckling resistance reduction caused by different boundary conditions of the elastic spherical shell. The elastic modulus is defined as E. The plastic reference resistance is derived in equation (3). The factor of C_{pl} is the factor that covers the buckling resistance reduction caused by different boundary conditions of an elastic-plastic spherical shell.

$$P_{Rpl} = \sigma_{Yield} C_{pl}\left(\frac{2t}{R}\right) \quad (3)$$

The spherical shell slenderness parameter λ is defined by equation (4).

$$\lambda = \sqrt{\frac{P_{Rpl}}{P_{Rcr}}} \quad (4)$$

The buckling reduction factors, χ should be determined as a function of relative slenderness of the spherical shell (i.e λ, λ_0 and λ_p) that can be expressed in equation (5).

$\chi = 0$ when $\lambda \leq \lambda_0$, $P_{ECCS} = P_{Rpl}$ (plastic)

$$\chi = 1 - \beta\left[\frac{\lambda - \lambda_o}{\lambda_p - \lambda_0}\right]^\eta \text{ when } \lambda_o \leq \lambda \leq \lambda_p \text{, elastic-plastic interaction} \tag{5}$$

$\chi = \frac{\alpha}{\lambda^2}$ when $\lambda_p \leq \lambda$, $P_{ECCS} = \alpha P_{Rk}$ (elastic)

The term α is the elastic imperfection reduction factor ('knock-down factor'), β is the plastic range factor, η is the interaction exponent which describes the shape of the elastic–plastic buckling interaction between λ_0 and λ_p. The term λ_0 is the squash limit slenderness. The term, λ_p is the plastic limit slenderness (i.e. the value of λ below which plasticity affects the stability) given by equation (6).

$$\lambda_p = \sqrt{\frac{\alpha}{1-\beta}} \tag{6}$$

The buckling pressure estimated by ECCS is expressed by equation (7) as the χ is referred to as the stability reduction factor.

$$P_{ECCS} = \chi P_{Rpl} \tag{7}$$

- The DnV (2013) design code estimated the collapse pressure as shown in equations (8) – (9)

$$\sigma_{cr} = \frac{\sigma_{Yield}}{\sqrt{1+\lambda^4}}$$

$$\lambda = \frac{\sigma_{Yield}}{\sqrt{\frac{0.606\rho E t}{R}}} \tag{8}$$

$$\rho = \frac{0.5}{\sqrt{1+\frac{R}{100t}}}$$

The terms are defined as the yield strength of the material, σ_{yield}, reduced slenderness, λ, and the imperfection factor, ρ. Therefore, the collapse pressure (P_{DnV}) is given by equation (9)

$$P_{DnV} = \frac{2t\sigma_{cr}}{R} \tag{9}$$

- The PD 5500 (2009) design code estimated the collapse pressure by referring to equation (10)

$$\left(\frac{1}{P_{PD\ 5500}}\right)^2 = \left(\frac{1}{0.3P_{cr}}\right)^2 + \left(\frac{1}{P_{yield}}\right)^2 \tag{10}$$

$$P_{Yield} = 2\sigma_{yield}\left(\frac{t}{R}\right) \tag{11}$$

The design pressure for the case of the spherical shell under elastic-plastic condition subjected to uniform external pressure is defined by P_{yield}. The P_{cr} and P_{yield} shall be determined in referring to equations (1) and (11), respectively. Usually, acceptable design pressure is controlled by the safety factor fitted to the test data. For the case of an externally pressurised spherical shell, the mean strength curve ($P_{PD\ 5500}$), PD 5500 adopts a safety factor of 1.75.

- The ABS (2021) design code estimated the collapse pressure by referring to equation (12)

$$P_{ABS} = 0.7391 P_{yield} \left[1 + \left(\frac{P_{yield}}{0.3P_{cr}}\right)^2\right]^{-\frac{1}{2}} \text{ For } \left(\frac{P_{cr}}{P_{yield}}\right) > 1 \quad (12)$$

$$P_{ABS} = 0.2124 P_{cr} \text{ For } \left(\frac{P_{cr}}{P_{yield}}\right) \leq 1$$

The collapse pressure is determined based on the ratio between elastic buckling pressure (P_{cr}) to the yield pressure (P_{yield}) from the equations (1) - (12). The mathematical expression is derived from the mean strength curve of the test model.

Table 1 summarised the experimental results of externally pressurised steel spherical shells with various geometries and a range of material properties. The experiment results are collected from the year 1994 to 2020 (26 years) with a population of 58 tested spherical shells. Table 1 also recorded the range of the dimensionless ratio of (i) radius-to-thickness, R/t of 43.078 <R/t< 1816.5, (ii) elastic Modulus, E of 150.8 GPa <E< 210 GPa, and (iii) yield stress, σ_{yield} 172.2 MPa <σ_{yield}< 335.408 MPa.

Table 1 Summary of recorded experiment data (i.e., geometrical and material properties) of spherical shell

R/t	E [GPa]	σ_{yield} [MPa]	Population	Year	Refs.
631.579	193	270	1	1994	(Jones, 1994)
137.258 - 450.286	200 - 210	172.2 - 420	7	1995	(Błachut and Galletly, 1995)
320.114 - 1816.5	207	303.5	6	2005	(Błachut, 2005)
43.078 - 111.322	183.1	237.9	6	2009	(Błachut, 2009)
79.140 - 80.526	159.208	335.408	6	2018	(Zhang et al., 2018)
324.753 - 1010.615	210	261.17 - 314.1	20	2018	(Kołodziej and Marcinowski, 2018)
82.218 - 83.333	159.208	335.408	3	2019	(Wang et al., 2020)
52.955 - 133.84	206	287 - 332	4	2020	(Cho et al., 2020)
77.922 - 78.947	150.8	313.63	5	2020	(Zhang et al., 2020)
		Total population	**58**		

The subsequent experimental data were screened and classified as 'thick shell', 'moderate shell', and 'thin shell' as follows:

- 'thick shell' - 40 ≤ R/t ≤ 100
- 'moderate shell' - 101 ≤ R/t ≤ 499
- 'thin shell' - R/t ≥ 500

3 RESULTS AND DISCUSSION

With practical interest in mind, a comparative evaluation of the design guidelines for buckling design of a steel spherical shell is performed. Tables 2 - 4 show a comparative analysis of the experimental data with the design guidelines for classified shells, as mentioned in the previous section. The magnitude of the experimental failure pressure is given in column three of each table (e.g. P_{exp}). The accuracy of the design codes is evaluated by the ratio of the experimental result to the calculated design code ($P_{exp}/P_{design\ code}$), which theoretically yields to be 1.0. The calculated values generally agree fairly with the experimental results. Alongside experimental buckling pressure, P_{exp}, the design codes are defined accordingly; (i) buckling pressure by ECCS, P_{ECCS}, (ii) buckling pressure by DnV, P_{DnV}, (iii) buckling pressure by PD 5500, $P_{PD\ 5500}$, and (iv) buckling pressure by ABS, P_{ABS}.

Table 2 shows a comparative analysis of the test data with different design codes for the case of 'thick shells" - 40 ≤ R/t ≤ 100. For the "thick shell" case, a total of 20 samples of spherical shells were provided. From the analysis, for the case of a thick shell, it is clear that DnV is the most reliable design code with an average P_{exp}/P_{DnV} of 1.037. Moreover, the DnV design code proves to be the most accurate for the case R/t = 87.101 with a ratio of experimental results to calculated design codes (i.e. P_{exp}/P_{DnV}) of 0.993. In contrast, for the case of R/t = 43.078, it is worth noting that PD 5500 produced a ratio closer to 1.0 (i.e $P_{exp}/ P_{PD\ 5500}$ = 0.979). On average, all the design codes underestimate the experimental result by nearly 3.6%.

Table 2 Comparison analysis of test data with design codes for 'thick shell' - 40 ≤ R/t ≤ 100

Sample	R/t	P_{exp}	P_{ECCS}	P_{DnV}	$P_{PD\ 5500}$	P_{ABS}	P_{exp}/P_{ECCS}	P_{exp}/P_{DnV}	$P_{exp}/P_{PD\ 5500}$	P_{exp}/P_{ABS}
1	83.333	5.077	4.941	6.333	5.779	4.271	1.028	0.802	0.879	1.189
2	82.613	5.036	5.002	6.414	5.854	4.326	1.007	0.785	0.860	1.164
3	82.218	5.709	5.036	6.459	5.895	4.357	1.134	0.884	0.968	1.310
4	80.525	5.280	4.566	5.835	5.322	3.933	1.156	0.905	0.992	1.342
5	79.520	5.553	4.650	5.947	5.424	4.009	1.194	0.934	1.024	1.385
6	79.367	5.255	4.663	5.964	5.439	4.020	1.127	0.881	0.966	1.307
7	79.826	5.580	4.624	5.913	5.392	3.985	1.207	0.944	1.035	1.400
8	79.140	5.356	4.682	5.990	5.463	4.038	1.144	0.894	0.980	1.327
9	79.596	5.647	4.644	5.938	5.416	4.003	1.216	0.951	1.043	1.411
10	87.461	5.490	4.021	5.795	5.489	4.057	1.365	0.947	1.000	1.353
11	52.955	9.810	8.141	10.379	10.042	7.422	1.205	0.945	0.977	1.322
12	77.922	8.690	8.518	6.553	5.997	4.432	1.020	1.326	1.449	1.961
13	78.947	8.720	8.276	6.433	5.884	4.349	1.054	1.356	1.482	2.005
14	78.947	8.470	8.276	6.433	5.884	4.349	1.023	1.317	1.439	1.947
15	78.947	8.920	8.276	6.433	5.884	4.349	1.078	1.387	1.516	2.051
16	77.922	9.470	8.518	6.553	5.997	4.432	1.112	1.445	1.579	2.137
17	44.254	9.460	16.124	10.483	10.259	7.582	0.587	0.902	0.922	1.248
18	43.078	10.340	17.102	10.785	10.564	7.808	0.605	0.959	0.979	1.324
19	85.129	5.930	7.659	5.006	4.785	3.537	0.774	1.185	1.239	1.677
20	87.101	4.830	3.640	4.865	4.648	3.435	1.327	0.993	1.039	1.406
						Average	**1.068**	**1.037**	**1.118**	**1.513**

Table 3 shows the comparative analysis of the test data with the design codes for the case of 'moderate shell' - 101 ≤ R/t ≤ 499. A total of 23 samples of tested spherical shells were recorded. The result clearly shows that PD 5500 design rule provides a better approach to estimating the buckling pressure with a ratio of P_{exp}/P_{DnV} = 1.098 to the tested shell. For the case of R/t = 101, PD 5500 overestimates the spherical buckling pressure by almost 6% corresponding with $P_{exp}/P_{PPD\ 5500}$ = 0.943. Besides that, PD 5500 estimates a much larger buckling load of about 30% for the case of R/t = 472. Overall, the average variances between the test data and the design code were found to be 8.9%.

Table 3 Comparison analysis of test data with design codes for 'moderate shell' - 101 ≤ R/t ≤ 499

Sample	R/t	P_{exp}	P_{ECCS}	P_{DnV}	$P_{PD\ 5500}$	P_{ABS}	P_{exp}/P_{ECCS}	P_{exp}/P_{DnV}	$P_{exp}/P_{PD\ 5500}$	P_{exp}/P_{ABS}
1	460	0.484	0.199	0.249	0.346	0.255	2.426	1.947	1.401	1.900
2	459	0.496	0.201	0.251	0.348	0.257	2.463	1.976	1.424	1.930
3	472	0.427	0.189	0.235	0.330	0.243	2.264	1.822	1.296	1.761
4	472	0.439	0.188	0.234	0.329	0.242	2.331	1.875	1.334	1.813
5	470	0.423	0.190	0.237	0.332	0.245	2.218	1.784	1.272	1.727
6	326	0.963	0.435	0.553	0.667	0.493	2.213	1.742	1.443	1.953
7	328	1.032	0.430	0.546	0.661	0.488	2.400	1.889	1.562	2.113
8	325	1.076	0.439	0.557	0.672	0.496	2.454	1.932	1.602	2.168
9	325	1.062	0.439	0.557	0.672	0.496	2.421	1.906	1.581	2.139
10	325	1.081	0.439	0.557	0.672	0.496	2.464	1.940	1.609	2.177
11	431	0.650	0.283	0.286	0.386	0.284	2.298	2.271	1.684	2.288
12	320	1.172	0.555	0.570	0.680	0.503	2.113	2.057	1.723	2.331
13	134	3.100	3.131	3.356	3.195	2.361	0.990	0.924	0.970	1.313
14	101	4.300	5.867	4.825	4.559	3.370	0.733	0.891	0.943	1.276
15	410	0.310	0.249	0.317	0.425	0.308	1.247	0.976	0.729	1.006
16	367	0.386	0.317	0.403	0.511	0.378	1.216	0.957	0.755	1.021
17	403	0.124	0.256	0.317	0.411	0.304	0.484	0.391	0.302	0.408
18	450	0.110	0.200	0.243	0.327	0.242	0.551	0.453	0.337	0.455
19	449	0.104	0.202	0.245	0.328	0.242	0.514	0.425	0.317	0.429
20	242	0.635	0.846	1.012	1.092	0.807	0.750	0.627	0.582	0.787
21	137	2.883	2.960	3.519	3.331	2.462	0.974	0.819	0.866	1.171
22	111	3.720	4.779	3.521	3.364	2.487	0.778	1.056	1.106	1.496
23	111	3.620	4.758	3.511	3.355	2.480	0.761	1.031	1.079	1.460
						Average	**1.825**	**1.329**	**1.098**	**1.475**

Table 4 shows the comparative analysis of the test data with the design codes for the case of "thin shell" case - R/t ≥ 500. From the tabulated results, a total of 15 specimens of buckled spherical shells were recorded. The present result shows a better agreement with the test results for the PD 5500 design rule with an average ratio of P_{exp}/ $P_{PPD\ 5500}$ = 1.844. With the corresponding ratio, it is seen that from the case of the 'thin shell', the PD 5500 design code overestimates the buckling load by means of more than 50%.

Table 4: Comparison analysis of test data with design codes for 'thin shell' - R/t ≥ 500

Sample	R/t	P_{exp}	P_{ECCS}	P_{DnV}	$P_{PD\ 5500}$	P_{ABS}	P_{exp}/ P_{ECCS}	P_{exp}/ P_{DnV}	P_{exp}/ $P_{PD\ 5500}$	P_{exp}/ P_{ABS}
1	632	0.132	0.112	0.108	0.172	0.124	1.180	1.227	0.767	1.061
2	998	0.098	0.034	0.038	0.076	0.054	2.860	2.553	1.296	1.811
3	1011	0.100	0.033	0.037	0.074	0.053	2.995	2.678	1.352	1.889
4	1001	0.100	0.034	0.038	0.075	0.054	2.934	2.619	1.328	1.856
5	1005	0.099	0.034	0.038	0.075	0.053	2.934	2.621	1.326	1.853
6	997	0.100	0.034	0.039	0.076	0.054	2.904	2.591	1.316	1.839
7	631	0.393	0.098	0.118	0.188	0.136	4.024	3.343	2.088	2.895
8	632	0.393	0.097	0.117	0.188	0.135	4.040	3.358	2.095	2.905
9	625	0.356	0.100	0.120	0.192	0.138	3.571	2.963	1.858	2.576
10	631	0.544	0.098	0.118	0.188	0.136	5.566	4.625	2.888	4.005
11	633	0.355	0.097	0.116	0.187	0.135	3.667	3.049	1.900	2.636
12	1817	0.046	0.011	0.009	0.023	0.016	4.302	5.276	2.028	2.858
13	1574	0.052	0.015	0.012	0.030	0.021	3.536	4.230	1.740	2.451
14	853	0.211	0.060	0.056	0.102	0.073	3.509	3.790	2.077	2.903
15	663	0.330	0.107	0.103	0.167	0.120	3.091	3.213	1.975	2.742
						Average	**3.621**	**3.412**	**1.844**	**2.570**

The results of prediction via the design code (ECCS, DnV, PD 5500, and ABS) are summarized in Tables 2 - 4. Overall, the prediction was empirically fit to the experimental data, with a few points worth highlighting here:

- The DnV (2013) design standard was found to be more appropriate in estimating the buckling load of the steel spherical shell for the 'thick shell' case
- For the case of 'moderate shell' and 'thin shell', the design code of PD 5500 (2009) was found to have good agreement with the experimental results
- In contrast, other design standards such as ECCS (2008) and ABS (2021) provide poor predictions (i.e. large discrepancies of buckling load estimation) for all shell categories tested
- Eventually, the discrepancy in the results can be associated with several factors, such as;
- the design recommendations proposed by the ECCS are somewhat too conservative for the case of 'moderate' and 'thin' shells, as reported by Kołodziej and Marcinowski (2018). This is because PD 5500 uses the mean curve rather than the lower bound used by ABS or ECCS design codes
- according to Cho et al. (2020), the empirical buckling load derived from a spherical shell is inconsistent when applied to a hemisphere, which is related to the uncertainties in the design codes used
- the residual stress and strain hardening derive from the welding and fabrication process needs to be accurately assessed as it shows a disparity in buckling load with a variance of 6% to 15% from the perfect shell. In addition, the combination of initial imperfection and uneven thickness reduces the collapse strength by up to 18%

The existing design code (ECCS, DnV, PD 5500, and ABS) practically plays an important role in the initial estimation of buckling load at the preliminary design stage. To note, improving the design formula to consider the effect of weld residual stress and stress relieving treatment is necessary to minimise the disparity of estimated buckling load.

Figure 2 shows the reliability results of the spherical shells calculated with the design code compared to the experimental results. The comparison was made with 58 test results of externally pressurised spherical shells with the current design codes (ECCS, DnV, PD 5500, and ABS). In this study, a statistical approach was taken by examining (i) the mean of the dimensionless ratio P_{exp}/P_{codes} of the collapse load from the experiment and the design codes, (ii) the coefficient of variation (COV), and (iii) the correlation between experiment and design code. Evidently some data points are found below the unity line, which indicates conservatism in estimating the buckling load by the design codes.

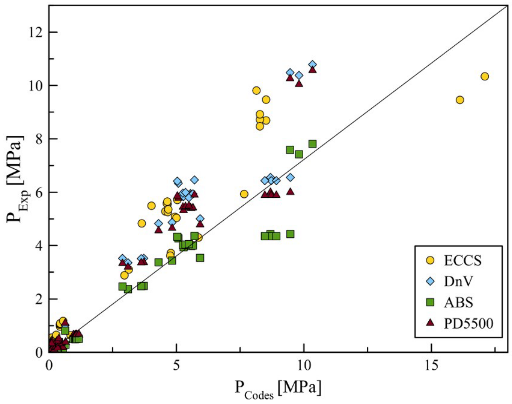

Figure 2: Comparison between experiment results against calculated design codes of externally pressurised spherical shells

Table 5 shows the statistical results of the externally pressurised steel spherical shells for a total of 58 samples of populations. The tabulated results clearly described the accuracy of the design code PD 5500 in estimating the collapse load of spherical shells, where the mean value of the dimensionless ratio, P_{exp}/P_{codes} near 1.0 with the value of COV was found to be P_{exp}/P_{codes} = 1.281 and COV = 9.383%. In contrast, other design codes such as ECCS, DnV, and ABS appear to be marginally in agreement with the experimental results with the mean value of the dimensionless ratio, P_{exp}/P_{codes}, and COV being found to be far off from 1.0.

Table 5 Statistical results of externally pressurised steel spherical shells

	ECCS	DnV	PD 5500	ABS
Mean, P_{exp}/P_{code}	1.889	1.734	1.281	1.753
COV [%]	11.917	10.122	9.383	6.937
Correlation	0.937	0.968	0.964	0.964
Total Population		58		

After further evaluation, 28 tested spherical shells subjected to external pressure were selected for a comparison analysis with lower bound curves in the format of PD 5500 and ECCS as shown in Figures 3 - 4. These test results were further evaluated as they produced a minimal disparity to the design curve derived from the guidelines. The selected test results are in the range of the dimensionless radius to thickness ratio, 43 <R/t <630, elastic modulus, 160 GPa <E< 210 GPa, and yield stress, 172 MPa <σ_{yield}< 420 MPa. Both figures use the ratio of the critical buckling pressure of the spherical shell in the elastic range and the buckling pressure of the spherical shell in the elastic-plastic range. Furthermore, Figure 4 indicates more conservative experimental results for 3 tested spherical shells as it is located below the ECCS curve (Błachut and Galletly, 1995), in comparison to the PD 5500 curve. The corresponding result shows PD 5500 design rule is more conservative as compared to the ECCS design code.

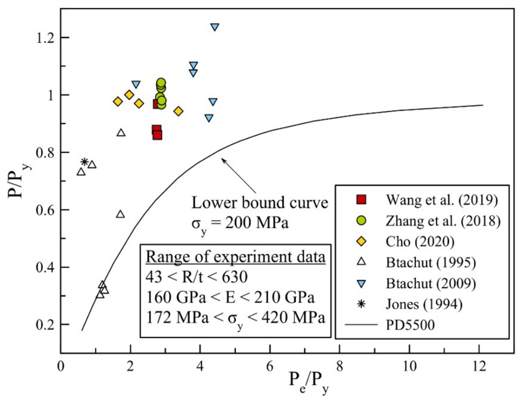

Figure 3: The experimental results of steel spherical shells subjected to external pressure in the format of PD 5500

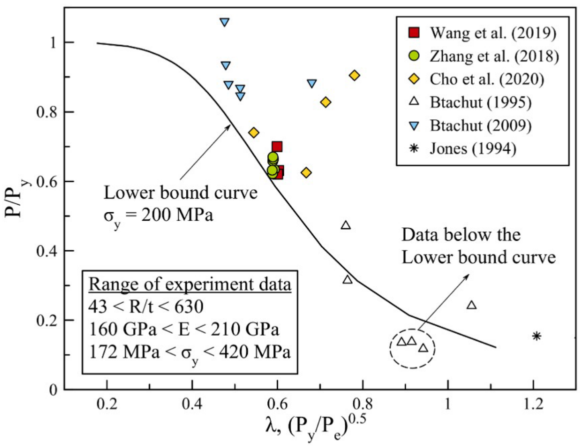

Figure 4: The experimental results of steel spherical shells subjected to external pressure in the format of ECCS

4 CONCLUSION

The present work deals with the comparative evaluation of the buckling capacity of steel spherical shells subjected to external pressure with the existing design rules. From the previous analysis, the following conclusions can be highlighted:

- On average, the comparative analysis clearly shows the DnV design code is well suited to estimate the buckling capacity of "thick shells" with a 3.6% deviation, while PD 5500 is more suitable for "medium and thin' shells with a deviation ranging from 9% to 50%.
- On the other hand, the statistical analysis shows that PD 5500 is close to 1.0 with the value of COV (i.e., 1.281 and 9.383%).
- After further evaluation, 28 shell test data were selected for comparison with the plotted curves in the format of PD 5500 and ECCS and agreed considerably well. Nevertheless, 3 test data were found to be below the lower limit curve specified in the design guideline for the ECCS.

As mentioned earlier, the discrepancies in the results can be associated with several factors, such as (i) the design recommendations proposed by the ECCS are somewhat too conservative for the case of 'moderate' and 'thin' shells, as PD 5500 uses the mean curve rather than the lower bound used by ABS or ECCS design codes, (ii) the empirical buckling load derived from a spherical shell is inconsistent when applied to a hemisphere, which is related to the uncertainties in the design codes used, and (iii) the presence of residual stresses and strain hardening in the actual experiment that can be derived from the fabrication and manufacturing processes, and the presence of imperfections that occur in the form of magnitude, location, and amplitude. Nevertheless, the design code plays an important role in the initial estimation of buckling load at the preliminary design stage.

The findings of the study can generally be very beneficial and significantly contribute to the understanding of the impacts of structural defects at the initial stages of design, construction, fabrication, and analysis of externally pressurised steel spherical shell structures.

Author’s Contributions: Conceptualization, MS Ismail; Methodology, MS Ismail; Investigation, MS Ismail; Writing - original draft, MS Ismail and J Mahmud; Writing - review & editing, MS Ismail and J Mahmud; Funding acquisition, J Mahmud; Resources, MS Ismail and J Mahmud; Supervision, MS Ismail and J Mahmud.

Editor: Pablo Andrés Muñoz Rojas

References

American Bureau of Shipping., 2021. Underwater Vehicles, Systems and Hyperbaric Facilities pp. 77 p. in various pagings.

Błachut, J., 2018. The Use of Composites in Underwater Pressure: Hull Components. Computational and Experimental Methods in Structures, 9, pp. 99–146.

Błachut, J., 2013. Combined stability of geometrically imperfect conical shells. Thin-Walled Structures, 67, pp. 121–128.

Błachut, J., 2009. Buckling of multilayered metal domes. Thin-Walled Structures, 47, pp. 1429–1438.

Błachut, J., 2005. Buckling of shallow spherical caps subjected to external pressure. Journal of Applied Mechanics, Transactions ASME, 72, pp. 803–806.

Błachut, J., Galletly, G.D., 1995. Buckling strength of imperfect steel hemispheres. Thin-Walled Structures, 23, pp. 1–20.

Błachut, J., Magnucki, K., 2008. Strength, Stability, and Optimization of Pressure Vessels: Review of Selected Problems. Applied Mechanics Reviews, 61, pp. 060801–1.

Błażejewski, P., Marcinowski, J. 2017. Comparisons of buckling capacity curves of pressurized spheres with EDR provisions and experimental results. Civil and Environmental Engineering Reports, 25, pp. 59 - 76

Cho, S.R., Muttaqie, T., Lee, S.H., Paek, J., Sohn, J.M., 2020. Ultimate Strength Assessment of Steel-Welded Hemispheres under External Hydrostatic Pressure. Journal of Marine Science and Application, 19, pp. 615–633.

DnV, 2013. DNV RP-C202: Buckling Strength of Shells. Det Norske Veritas AS, pp. 27.

ECCS, 2008. Buckling of steel shells european design recommendations. Buckling of Shells 5th Ed Brussels: European Convention for Constructional Steelwork.

Ifayefunmi, O., 2016. Buckling behavior of axially compressed cylindrical shells: Comparison of theoretical and experimental data. Thin-Walled Structures, 98, pp. 558–564.

Ifayefunmi, O., Ismail, M.S., Othman, M.Z.A. 2021. Buckling of unstiffened cone-cylinder shells subjected to axial compression and thermal loading. Ocean Engineering, 225, pp. 108601.

Ismail, M.S., Purbolaksono, J., Muhammad, N., Andriyana, A., Liew, H.L. 2015. Statistical analysis of imperfection effect on cylindrical buckling response. IOP Conference Series: Materials Science and Engineering, 100, pp. 012003

Ismail, M.S., 2023. Buckling of an imperfect spherical shell subjected to external pressure. Ocean Engineering, 275, pp. 114118

Jasion, P., Magnucki, K., 2015. Elastic buckling of Cassini ovaloidal shells under external pressure - Theoretical study. Archives of Mechanics, 67, pp. 179–192.

Jones, D.R.H., 1994. Buckling failures of pressurised vessels-two case studies. Engineering Failure Analysis, 1, pp. 155–167.

Kołodziej, S., Marcinowski, J., 2018. Experimental and numerical analyses of the buckling of steel, pressurized, spherical shells. Advances in Structural Engineering, 21, pp. 2416–2432.

Pan, B.B., Cui, W., Shen, Y.S., Liu, T., 2010. Further study on the ultimate strength analysis of spherical pressure hulls. Marine Structures, 23, pp. 444–461.

PD 5500, 2009. Specification for unfired fusion welded pressure vessels This publication is not to be regarded as a British Standard. pp. 904.

Sofiyev, A., Aksogan, O., Schnack, E., Avcar, M. 2008. The stability of a three-layered composite conical shell containing a FGM layer subjected to external pressure. Mechanics of Advanced Materials and Structures, 6-7, pp. 461-466.

Tripathi, S.M., Anup, S., Muthukumar, R., 2016. Effect of geometrical parameters on mode shape and critical buckling load of dished shells under external pressure. Thin-Walled Structures, 106, pp. 218–227.

Wagner, H.N.R., Hühne, C., Niemann, S., 2018. Robust knockdown factors for the design of spherical shells under external pressure: development and validation. International Journal of Mechanical Sciences, 141, pp. 58–77.

Wang, L.R.L., 1967. Discrepancy of Experimental Buckling Pressures of Spherical Shells. AIAA Journal, 5:2, pp. 357-359

Wang, Y., Zhang, J., Tang, W., 2020. Buckling Performances of Spherical Caps Under Uniform External Pressure. Journal of Marine Science and Application, 19, pp. 96–100.

Zhang, J., Huang, C., Wagner, H.N.R., Cui, W., Tang, W., 2020. Study on dented hemispheres under external hydrostatic pressure. Marine Structures, 74, pp. 102819.

Zhang, J., Wang, Y., Wang, F., Tang, W., 2018. Buckling of stainless steel spherical caps subjected to uniform external pressure. Ships and Offshore Structures, 13, pp. 779–785.

Zhang, J., Zhang, M., Tang, W., Wang, W., Wang, M., 2017. Buckling of spherical shells subjected to external pressure: A comparison of experimental and theoretical data. Thin-Walled Structures, 111, pp. 58–64.

Zhang, J., Zhang, Y., Wang, F., Zhu, Y.M., Cui, W.C., Chen, Y., Jiang, Z., 2019. Experimental and numerical studies on the buckling of the hemispherical shells made of maraging steel subjected to extremely high external pressure. International Journal of Pressure Vessels and Piping, 172, pp. 56–64.

Zhu, Y., Zhang, Y., Zhao, X., Zhang, J., Xu, X., 2019. Elastic–plastic buckling of externally pressurised hemispherical heads. Ships and Offshore Structures, 14, pp. 829–838.

Zoelly, R., 1915. Uber ein Knickungsproblem an der Kugelschale. Ph.D Thesis. ETH Zurich.